
M. AYGUN

Department of Physics, Bitlis Eren University
(Bitlis, Turkey; e-mail: murata.25@gmail.com)

EFFECTS OF PROXIMITY POTENTIALS ON THE CROSS-SECTIONS OF ${}^{6,8}\text{He} + {}^{65}\text{Cu}$ HALO FUSION REACTIONS

UDC 539

The comprehensive theoretical study is performed to determine the best proximity potentials in reproducing ${}^{6,8}\text{He} + {}^{65}\text{Cu}$ fusion reactions. Twenty three different versions of proximity potentials that consist of Prox 66, Prox 76, Prox 77, Prox 79, Prox 81-I, Prox 81-II, Prox 81-III, Prox 84, Prox 88, Mod-Prox-88, Prox 95, Prox 2003-I, Prox 2003-II, Prox 2003-III, Prox 2010, BW 91, AW 95, Bass 73, Bass 77, Bass 80, CW 76, Ngo 80, and D are used. The theoretical results are compared with experimental data on ${}^{6,8}\text{He} + {}^{65}\text{Cu}$ fusion reactions. The appropriate proximity potentials are determined.

Keywords: fusion cross-sections, proximity potentials, halo nuclei.

1. Introduction

Studies of halo nuclei are still a current topic in the field of nuclear physics. It is well known that the parameters such as the binding energy, isospin values, wave function(s) of the valence nucleon(s), and density distributions are different for the halo nuclei; ${}^6\text{He}$, ${}^8\text{He}$, ${}^{11}\text{Li}$, ${}^{11}\text{Be}$, ${}^{14}\text{Be}$, ${}^{14}\text{B}$, ${}^{15}\text{C}$, and ${}^{19}\text{C}$ are accepted to be neutron halo nuclei; ${}^6\text{He}$ and ${}^8\text{He}$ are among the most important of these nuclei. In addition to the elastic scattering interactions of these nuclei, the fusion reactions are also an important issue. In this context, Navin et al. [1] have presented the data on ${}^6\text{He} + {}^{65}\text{Cu}$ fusion reaction. Chatterjee et al. [2] the displayed exclusive measurement of fusion ${}^6\text{He}$ by ${}^{65}\text{Cu}$. Then the fusion cross-section of ${}^8\text{He} + {}^{65}\text{Cu}$ reaction has been reported by Lemasson et al. [3]. Both theoretical and experimental studies for understanding the fusion processes of halo nuclei ${}^6\text{He}$ [4–7] and ${}^8\text{He}$ [8, 9] can be found in the literature.

The nucleus-nucleus potentials are very important to study the fusion reactions of halo nuclei. For this purpose, different potentials such as those in the dou-

ble folding model [10], time-dependent Hartree–Fock theory [11], and model with Skyrme energy-density functional [12] can be evaluated. In addition, proximity potentials are of importance in obtaining the nuclear potentials of fusion reactions. The alpha decay process [13], cluster decay process [14], fission reaction [15], and elastic scattering reactions [16–19] have been examined, by using these potentials. On the other hand, it can be seen, while the literature is examined, that the fusion reactions of ${}^6\text{He}$ and ${}^8\text{He}$ nuclei have not been analyzed, by using a wide range of proximity potentials. Therefore, we consider that it will be useful and interesting to overcome this deficiency in the literature for ${}^6\text{He}$ and ${}^8\text{He}$ halo nuclei which are isotopes with each other.

In the present study, we will examine the effects of the proximity potentials on ${}^6\text{He} + {}^{65}\text{Cu}$ and ${}^8\text{He} + {}^{65}\text{Cu}$ fusion cross-sections. It would be interesting to compare the fusion results of two halo nuclei with the neutron rich isotopes over the same target nucleus. With this goal, we apply twenty three different types of proximity potentials to obtain the fusion cross-sections, which can be emphasized as proximity 1966, proximity 1976, proximity 1977, proximity

1979, proximity 1981-I, proximity 1981-II, proximity 1981-III, proximity 1984, proximity 1988, modified proximity 1988, proximity 1995, proximity 2003-I, proximity 2003-II, proximity 2003-III, proximity 2010, Broglia and Winther 1991, Aage Winther, and Bass 1973, Bass 1977, Bass 1980, Christensen and Winther 1976, Ngo 1980, and Denisov potential. Then we compare the theoretical results and experimental data.

Section 2 gives a brief description of proximity potentials used in the theoretical calculations. Section 3 presents the calculation procedure. Section 4 shows the results and the discussion of calculations. Section 5 provides the summary and conclusion.

2. Proximity Potentials

In the theoretical analysis of fusion cross sections of ${}^6,8\text{He} + {}^{65}\text{Cu}$ reactions, we apply twenty three different versions of proximity potentials. These potentials are explained in the following subsections.

2.1. Prox 66, Prox 76, Prox 77, Prox 79, Prox 81, Prox 84, Prox 88, Mod-Prox-88, Prox 95, Prox 2003, Prox 2010 potentials

Prox 77 version of the proximity potential [20, 21] is in the following form:

$$V_N^{\text{Prox 77}}(r) = 4\pi\gamma b \bar{R} \Phi \left(\zeta = \frac{r - C_1 - C_2}{b} \right) \text{ MeV}, \quad (1)$$

where

$$\bar{R} = \frac{C_1 C_2}{C_1 + C_2}, \quad C_i = R_i \left[1 - \left(\frac{b}{R_i} \right)^2 + \dots \right], \quad b \approx 1 \text{ fm}, \quad (2)$$

R_i (effective radius) has the form

$$R_i = 1.28A_i^{1/3} - 0.76 + 0.8A_i^{-1/3} \text{ fm} \quad (i = 1, 2), \quad (3)$$

and γ (surface energy coefficient) is taken as

$$\gamma = \gamma_0 \left[1 - k_s \left(\frac{N - Z}{N + Z} \right)^2 \right], \quad (4)$$

where $N(Z)$ is the total number of neutrons(protons). The universal function $\Phi(\zeta)$ is evaluated as

$$\Phi(\zeta) = \begin{cases} -\frac{1}{2}(\zeta - 2.54)^2 - 0.0852(\zeta - 2.54)^3 & \text{for } \zeta \leq 1.2511, \\ -3.437 \exp\left(-\frac{\zeta}{0.75}\right) & \text{for } \zeta \geq 1.2511. \end{cases}$$

362

Table 1. γ_0 and k_s values of Prox 66, Prox 76, Prox 77, Prox 79, Prox 81, Prox 84, Prox 88, Mod-Prox-88, Prox 95, Prox 2003, and Prox 2010 potentials

Potential type	γ_0 , MeV/fm ²	k_s	Ref.
Prox 66	1.01734	1.79	[22]
Prox 76	1.460734	4.0	[23]
Prox 77	0.9517	1.7826	[22]
Prox 79	1.2402	3.0	[24]
Prox 81-I	1.1756	2.2	[25]
Prox 81-II	1.27326	2.5	[25]
Prox 81-III	1.2502	2.4	[25]
Prox 84	0.9517	2.6	[26]
Prox 88	1.2496	2.3	[27]
Mod-Prox-88	1.65	2.3	[28]
Prox 95	1.25284	2.345	[29]
Prox 2003-I	1.08948	1.9830	[30]
Prox 2003-II	0.9180	0.7546	[30]
Prox 2003-III	0.911445	2.2938	[30]
Prox 2010	1.460734	4.0	[21, 31, 32]

Then a lot of studies have been performed on the proximity potentials. Different values of γ_0 and k_s have been proposed as a result of these studies. The other parameters of these potentials are the same as for Prox 77 potential. In this context, there are fifteen various potentials examined in this work. The γ_0 and k_s values of these potentials values are given in Table 1.

2.2. Broglia and Winther 1991 (BW 91) potential

BW 91 potential [27] is used as [33]

$$V_N^{\text{BW 91}}(r) = -\frac{V_0}{[1 + \exp\left(\frac{r-R_0}{a}\right)]} \text{ MeV}, \quad (5)$$

where

$$V_0 = 16\pi \frac{R_1 R_2}{R_1 + R_2} \gamma a, \quad a = 0.63 \text{ fm}, \quad (6)$$

and

$$\begin{aligned} R_0 &= R_1 + R_2 + 0.29, \\ R_i &= 1.233A_i^{1/3} - 0.98A_i^{-1/3} \quad (i = 1, 2), \end{aligned} \quad (7)$$

where γ , γ_0 , and k_s , are, respectively,

$$\gamma = \gamma_0 \left[1 - k_s \left(\frac{N_p - Z_p}{A_p} \right) \left(\frac{N_t - Z_t}{A_t} \right) \right], \quad (8)$$

$$\gamma_0 = 0.95 \text{ MeV/fm}^2, \quad k_s = 1.8.$$

2.3. Aage Winther (AW 95) potential

The only difference between AW 95 and BW 91 potentials [33, 34] is

$$a = \left[\frac{1}{1.17(1 + 0.53(A_1^{-1/3} + A_2^{-1/3}))} \right] \text{ fm}, \quad (9)$$

and

$$R_0 = R_1 + R_2, \quad R_i = 1.2A_i^{1/3} - 0.09 \quad (i = 1, 2). \quad (10)$$

2.4. Bass 1973 (Bass 73) potential

A different version of the proximity potentials from [35, 36] is Bass 73 potential given by [21]

$$V_N^{\text{Bass 73}}(r) = -\frac{da_s A_1^{1/3} A_2^{1/3}}{R_{12}} \exp\left(-\frac{r - R_{12}}{d}\right) \text{ MeV}, \quad (11)$$

where

$$R_{12} = 1.07(A_1^{1/3} + A_2^{1/3}), \quad d = 1.35 \text{ fm}, \quad a_s = 17 \text{ MeV}. \quad (12)$$

2.5. Bass 1977 (Bass 77) potential

Bass 77 potential [37] is considered as [33]

$$V_N^{\text{Bass 77}}(s) = -\frac{R_1 R_2}{R_1 + R_2} \phi(s = r - R_1 - R_2) \text{ MeV}, \quad (13)$$

where

$$R_i = 1.16A_i^{1/3} - 1.39A_i^{-1/3} \quad (i = 1, 2). \quad (14)$$

The universal function $\phi(s = r - R_1 - R_2)$ is parametrized by

$$\phi(s) = \left[A \exp\left(\frac{s}{d_1}\right) + B \exp\left(\frac{s}{d_2}\right) \right]^{-1}, \quad (15)$$

where $A = 0.030 \text{ MeV}^{-1} \text{ fm}$, $B = 0.0061 \text{ MeV}^{-1} \text{ fm}$, $d_1 = 3.30 \text{ fm}$, and $d_2 = 0.65 \text{ fm}$.

2.6. Bass 1980 (Bass 80) potential

The difference between Bass 80 and Bass 77 potentials is the function $\phi(s = r - R_1 - R_2)$ shown by [27, 33]

$$\phi(s) = \left[0.033 \exp\left(\frac{s}{3.5}\right) + 0.007 \exp\left(\frac{s}{0.65}\right) \right]^{-1}, \quad (16)$$

and

$$R_i = R_s \left(1 - \frac{0.98}{R_s^2} \right), \quad (17)$$

$$R_s = 1.28A_i^{1/3} - 0.76 + 0.8A_i^{-1/3} \text{ fm} \quad (i = 1, 2).$$

2.7. Christensen and Winther 1976 (CW 76) potential

CW 76 potential [38] is parametrized by [21]

$$V_N^{\text{CW 76}}(r) = -50 \frac{R_1 R_2}{R_1 + R_2} \phi(r - R_1 - R_2) \text{ MeV}, \quad (18)$$

where

$$R_i = 1.233A_i^{1/3} - 0.978A_i^{-1/3} \text{ fm} \quad (i = 1, 2). \quad (19)$$

The universal function $\phi(s = r - R_1 - R_2)$ is

$$\phi(s) = \exp\left(-\frac{r - R_1 - R_2}{0.63}\right). \quad (20)$$

2.8. Ngô 1980 (Ngo 80) potential

The Ngo 80 form of a proximity potential is formulated by [39]

$$V_N^{\text{Ngo 80}}(r) = \bar{R} \phi(r - C_1 - C_2) \text{ MeV}, \quad (21)$$

$$\bar{R} = \frac{C_1 C_2}{C_1 + C_2}, \quad C_i = R_i \left[1 - \left(\frac{b}{R_i} \right)^2 + \dots \right], \quad (22)$$

$$R_i = \frac{NR_{ni} + ZR_{pi}}{A_i} \quad (i = 1, 2), \quad (23)$$

$$R_{pi} = r_{0pi} A_i^{1/3}, \quad R_{ni} = r_{0ni} A_i^{1/3}, \quad (24)$$

$$r_{0pi} = 1.128 \text{ fm}, \quad r_{0ni} = 1.1375 + 1.875 \times 10^{-4} A_i \text{ fm}. \quad (25)$$

The universal function $\phi(s = r - C_1 - C_2)$ (in MeV/fm) takes the form

$$\Phi(s) = \begin{cases} -33 + 5.4(s - s_0)^2, & \text{for } s < s_0, \\ -33 \exp\left[-\frac{1}{5}(s - s_0)^2\right] & \text{for } s \geq s_0, \\ s_0 = -1.6 \text{ fm}. \end{cases}$$

2.9. Denisov (D) potential

D potential evaluated in the analysis of fusion reactions is given by [33, 40]

$$V_N^D(r) = -1.989843 \frac{R_1 R_2}{R_1 + R_2} \phi(r - R_1 - R_2 - 2.65) \times$$

$$\times \left[1 + 0.003525139 \left(\frac{A_1}{A_2} + \frac{A_2}{A_1} \right)^{3/2} - 0.4113263(I_1 + I_2) \right] \text{ MeV}, \quad (26)$$

where

$$I_i = \frac{N_i - Z_i}{A_i}, \quad (27)$$

and

$$R_i = R_{ip} \left(1 - \frac{3.413817}{R_{ip}^2} \right) + 1.284589 \left(I_i - \frac{0.4A_i}{A_i + 200} \right), \quad (28)$$

$$R_{ip} = 1.24A_i^{1/3} \left(1 + \frac{1.646}{A_i} - 0.191 \left(\frac{A_i - 2Z_i}{A_i} \right) \right) \quad (i = 1, 2). \quad (29)$$

The function $\phi(s = r - R_1 - R_2 - 2.65)$ is considered as

$$\phi(s) = \begin{cases} 1 - \frac{s}{0.7881663} + 1.229218s^2 - 0.2234277s^3 - \\ - 0.1038769s^4 - \frac{R_1R_2}{R_1 + R_2} (0.1844935s^2 + \\ + 0.07570101s^3 + (I_1 + I_2)(0.04470645s^2 + \\ + 0.0334687s^3)) \quad (-5.65 \leq s \leq 0), \\ \left(1 - s^2 \left(0.05410106 \frac{R_1R_2}{R_1 + R_2} \exp\left(-\frac{s}{1.76058}\right) - \right. \right. \\ \left. \left. - 0.539542(I_1 + I_2) \exp\left(-\frac{s}{2.424408}\right) \right) \right) \times \\ \times \exp\left(-\frac{s}{0.7881663}\right) \quad (s \geq 0). \end{cases}$$

3. Calculation Procedure

In the present study, the total interaction potential can be assumed as

$$V_{\text{total}}(r) = V_C(r) + V_N(r), \quad (30)$$

where V_C is the Coulomb potential shown by [41]

$$V_C(r) = \frac{1}{4\pi\epsilon_0} \frac{Z_P Z_T e^2}{r}, \quad r \geq R_c \quad (31)$$

$$= \frac{1}{4\pi\epsilon_0} \frac{Z_P Z_T e^2}{2R_c} \left(3 - \frac{r^2}{R_c^2} \right), \quad r < R_c \quad (32)$$

$$R_c = 1.25(A_P^{1/3} + A_T^{1/3}), \quad (33)$$

and V_N is the nuclear potential. The real part of the nuclear potential is acquired by using twenty three different versions of a proximity potential. These potentials have been clearly defined in the subsections

above. The imaginary part of the nuclear potential is taken as the Woods-Saxon potential shown by

$$W(r) = \frac{W_0}{\left[1 + \exp\left(\frac{r - R_w}{a_w}\right) \right]}, \quad R_w = r_w(A_P^{1/3} + A_T^{1/3}), \quad (34)$$

where W_0 is the potential depth, r_w is the radius parameter, a_w is the diffuseness parameter, and A_P (A_T) is the mass of a projectile (target) nucleus, respectively. The code FRESKO is used in the calculations of fusion cross-sections [42].

4. Results and Discussion

As the first step, we have calculated the nuclear parts of the total interaction potentials of ${}^6\text{He} + {}^{65}\text{Cu}$ and ${}^8\text{He} + {}^{65}\text{Cu}$ systems. With this goal, we have achieved the real parts of nuclear potentials, by using twenty three different proximity potentials such as Prox 66, Prox 76, Prox 77, Prox 79, Prox 81-I, Prox 81-II, Prox 81-III, Prox 84, Prox 88, Mod-Prox-88, Prox 95, Prox 2003-I, Prox 2003-II, Prox 2003-III, Prox 2010, BW 91, AW 95, Bass 73, Bass 77, Bass 80, CW 76, Ngo 80, and D ones. The distance-dependent variations of the real parts of nuclear potentials have been displayed in Fig. 1. Then we have applied the Woods-Saxon potential for the imaginary parts of the nuclear potentials of ${}^6\text{He} + {}^{65}\text{Cu}$ and ${}^8\text{He} + {}^{65}\text{Cu}$ reactions. We have set free the W_0 , r_w and a_w parameters of the imaginary potential in order to obtain agreement of the theoretical results with the experimental data. We have listed the values of W_0 , r_w , and a_w used in the calculations in Tables 2 and 3. When we examine the values of the imaginary potential parameters from Tables 2 and 3, we observe that the imaginary part of the nucleus-nucleus potential in obtaining the cross-sections of fusion reactions has a strong effect on the results.

The fusion cross-sections of ${}^6\text{He} + {}^{65}\text{Cu}$ reaction have been shown as a function of the center-of-mass energy in Fig. 2. The potential parameters of the imaginary part of the nuclear potential have been given in Table 2. It has been observed that the theoretical results of the proximity potentials except for Bass 73 potential are very similar to each other. The results of other potentials are more smooth and the result of the Bass 73 proximity potential is more oscillating. This makes the result of the Bass 73 potential

even better than other potentials. It can be said that different versions of proximity potentials applied in this work can explain the experimental data on the ${}^6\text{He} + {}^{65}\text{Cu}$ fusion cross-section.

The fusion cross-sections of the ${}^8\text{He} + {}^{65}\text{Cu}$ system have been obtained, by using twenty three different potentials. The results have been compared with the experimental data as a function of the center-of-mass energy in Fig. 3. Additionally, the imaginary potential parameters of the nuclear potential have been listed in Table 3. Similarly to the results of ${}^6\text{He} + {}^{65}\text{Cu}$ reaction, the results of ${}^8\text{He} + {}^{65}\text{Cu}$ reaction except for Bass 73 potential are very close to one another. The results are in a very good agreement with the exper-

Table 2. The potential parameters W_0 (in MeV), r_w (in fm) and a_w (in fm) used in the calculations of the fusion cross-sections of ${}^6\text{He}$ on ${}^{65}\text{Cu}$ target nucleus, by using Prox 66, Prox 76, Prox 77, Prox 79, Prox 81-I, Prox 81-II, Prox 81-III, Prox 84, Prox 88, Mod-Prox-88, Prox 95, Prox 2003-I, Prox 2003-II, Prox 2003-III, Prox 2010, BW 91, AW 95, Bass 73, Bass 77, Bass 80, CW 76, Ngo 80, and D potentials

Reaction ${}^6\text{He} + {}^{65}\text{Cu}$	W (MeV)	r_w (fm)	a_w (fm)
Prox 66	15.0	0.9	0.82
Prox 76	15.0	0.9	0.50
Prox 77	15.0	0.9	0.83
Prox 79	15.0	0.9	0.60
Prox 81-I	15.0	0.9	0.70
Prox 81-II	15.0	0.9	0.60
Prox 81-III	15.0	0.9	0.63
Prox 84	15.0	0.9	0.80
Prox 88	25.0	0.9	0.55
Mod-Prox-88	7.00	0.9	0.50
Prox 95	25.0	0.9	0.60
Prox 2003-I	25.0	0.9	0.70
Prox 2003-II	25.0	0.9	0.76
Prox 2003-III	25.0	0.9	0.75
Prox 2010	10.0	0.9	0.50
BW 91	8.80	0.9	0.50
AW 95	5.00	0.9	0.50
Bass 73	4.60	0.9	0.50
Bass 77	19.0	0.9	0.80
Bass 80	4.10	0.9	0.50
CW 76	37.0	0.9	0.50
Ngo 80	17.0	0.9	0.85
D	35.0	0.9	0.87

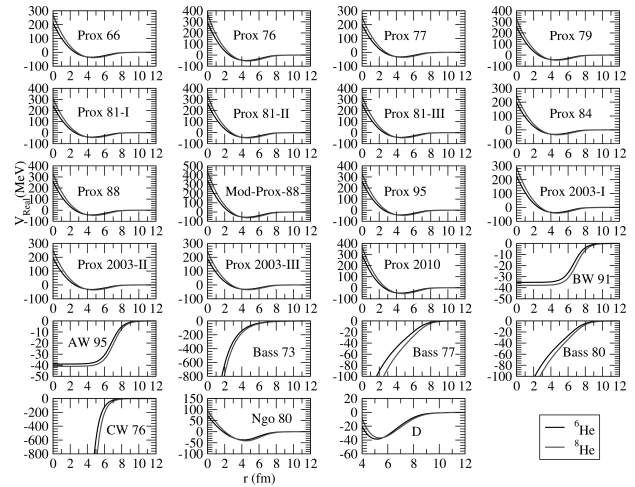


Fig. 1. Distance-dependent changes of the real parts of the nuclear potentials for Prox 66, Prox 76, Prox 77, Prox 79, Prox 81-I, Prox 81-II, Prox 81-III, Prox 84, Prox 88, Mod-Prox-88, Prox 95, Prox 2003-I, Prox 2003-II, Prox 2003-III, Prox 2010, BW 91, AW 95, Bass 73, Bass 77, Bass 80, CW 76, Ngo 80, and D ones

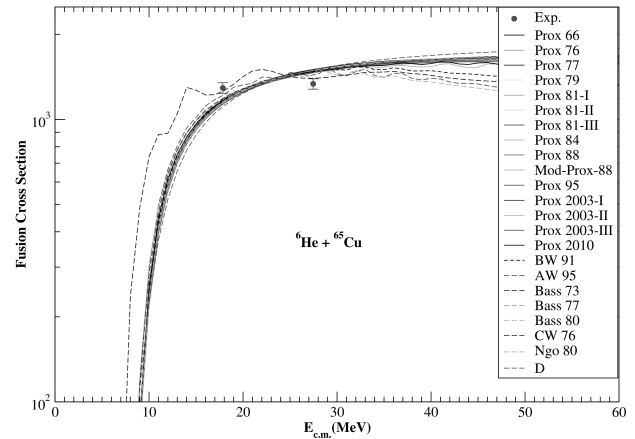


Fig. 2. Fusion cross-sections of ${}^6\text{He} + {}^{65}\text{Cu}$ reaction in comparison with the experimental data, by using Prox 66, Prox 76, Prox 77, Prox 79, Prox 81-I, Prox 81-II, Prox 81-III, Prox 84, Prox 88, Mod-Prox-88, Prox 95, Prox 2003-I, Prox 2003-II, Prox 2003-III, Prox 2010, BW 91, AW 95, Bass 73, Bass 77, Bass 80, CW 76, Ngo 80, and D potentials. The experimental data are taken from Ref. [1]

imental data. Unlike ${}^6\text{He} + {}^{65}\text{Cu}$ reaction, the results with Bass 73 potential for ${}^8\text{He} + {}^{65}\text{Cu}$ reaction are not better than other potentials. It can be concluded that the proximity potentials evaluated in this study can provide a good agreement with the experimental data on ${}^6\text{He} + {}^{65}\text{Cu}$ fusion cross-section.

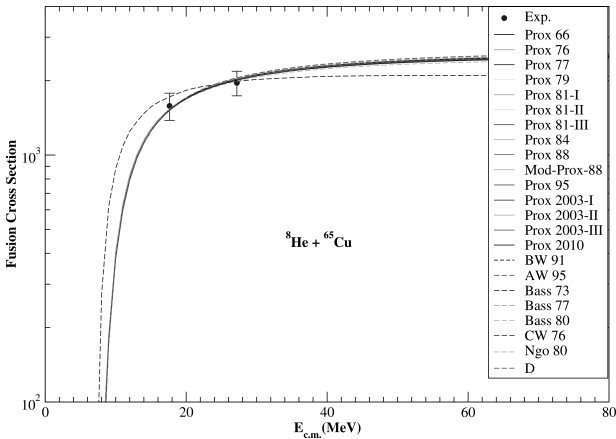


Fig. 3. Fusion cross-sections of $^8\text{He} + ^{65}\text{Cu}$ reaction in comparison with the experimental data, by using Prox 66, Prox 76, Prox 77, Prox 79, Prox 81-I, Prox 81-II, Prox 81-III, Prox 84, Prox 88, Mod-Prox-88, Prox 95, Prox 2003-I, Prox 2003-II, Prox 2003-III, Prox 2010, BW 91, AW 95, Bass 73, Bass 77, Bass 80, CW 76, Ngo 80, and D potentials. The experimental data are taken from Ref. [3]

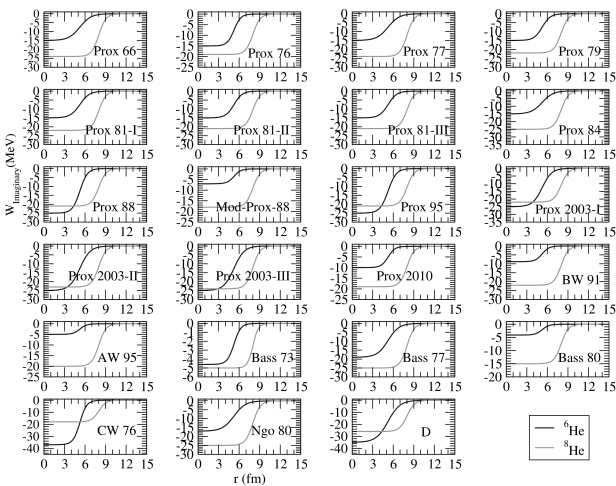


Fig. 4. Distance-dependent changes of the imaginary parts of nuclear potentials for Prox 66, Prox 76, Prox 77, Prox 79, Prox 81-I, Prox 81-II, Prox 81-III, Prox 84, Prox 88, Mod-Prox-88, Prox 95, Prox 2003-I, Prox 2003-II, Prox 2003-III, Prox 2010, BW 91, AW 95, Bass 73, Bass 77, Bass 80, CW 76, Ngo 80, and D potentials

By carefully examining Figs. 2 and 3, we can notice that the cross-sections of $^6\text{He} + ^{65}\text{Cu}$ reaction show the appearance of wobbling, while the cross-sections of $^8\text{He} + ^{65}\text{Cu}$ do not present it. ^8He nucleus has a $4n + \text{core}$ configuration, and ^6He nucleus displays the

Table 3. The same as in Table 2, but for $^8\text{He} + ^{65}\text{Cu}$ reaction

Reaction $^8\text{He} + ^{65}\text{Cu}$	W (MeV)	r_ω (fm)	a_ω (fm)
Prox 66	24.0	1.33	0.53
Prox 76	19.0	1.33	0.53
Prox 77	24.0	1.33	0.53
Prox 79	22.0	1.33	0.53
Prox 81-I	22.0	1.33	0.53
Prox 81-II	21.0	1.33	0.53
Prox 81-III	21.0	1.33	0.53
Prox 84	25.0	1.33	0.53
Prox 88	21.0	1.33	0.53
Mod-Prox-88	18.0	1.33	0.53
Prox 95	21.0	1.33	0.53
Prox 2003-I	22.0	1.33	0.53
Prox 2003-II	23.0	1.33	0.53
Prox 2003-III	24.0	1.33	0.53
Prox 2010	19.0	1.33	0.53
BW 91	22.0	1.33	0.53
AW 95	20.0	1.33	0.53
Bass 73	5.00	1.33	0.40
Bass 77	25.0	1.33	0.53
Bass 80	15.0	1.33	0.53
CW 76	18.0	1.33	0.53
Ngo 80	25.0	1.33	0.55
D	26.0	1.33	0.56

$2n + \text{core}$ configuration. This leads to the differentiation in the binding energies of ^6He and ^8He nuclei. As a result, we think that $^6\text{He} + ^{65}\text{Cu}$ reaction displays a wobble structure as compared to $^8\text{He} + ^{65}\text{Cu}$ reaction. In other words, we can say that the structural differences of ^6He and ^8He nuclei cause differences in the cross-sections.

The distance-dependent changes of imaginary potentials of ^6He and ^8He nuclei have been also displayed in Fig. 4. When the depths of the imaginary potentials are examined, it is observed that the potential depth of ^8He nucleus is generally deeper than that of ^6He nucleus. Additionally, it is seen that ^6He nucleus goes to zero faster than ^8He nucleus. It can be said that ^8He nucleus is more attractive and diffusive than ^6He nucleus.

5. Summary and Conclusions

In this study, we have investigated the effects of twenty three different versions of proximity poten-

tials on the fusion cross sections of ${}^6\text{He} + {}^{65}\text{Cu}$ and ${}^8\text{He} + {}^{65}\text{Cu}$ reactions. It has been seen that the proximity potentials have given a good agreement results with experimental data. It has been observed that the fusion cross-sections of ${}^6\text{He} + {}^{65}\text{Cu}$ and ${}^8\text{He} + {}^{65}\text{Cu}$ systems slightly depend on the shapes of proximity potentials. In addition, it has been noticed that Bass 73 potential in the ${}^6\text{He} + {}^{65}\text{Cu}$ fusion reaction is slightly better matched to experimental data than other proximity potentials. It has been observed that the results obtained with proximity potentials of ${}^8\text{He} + {}^{65}\text{Cu}$ fusion reaction, except for Bass 73 potential, are very similar to one another.

Consequently, it can be concluded that different versions of proximity potentials applied in the present work are highly applicable in explaining the experimental data of both ${}^6\text{He} + {}^{65}\text{Cu}$ and ${}^8\text{He} + {}^{65}\text{Cu}$ fusion cross-sections. We can say also that the proximity potentials will be interesting in explaining other fusion reactions.

The author would like to thank the anonymous Referee for valuable comments.

1. A. Navin, V. Tripathi, Y. Blumenfeld, V. Nanal, C. Simenel, J.M. Casandjian, G. de France, R. Raabe, D. Bazin, A. Chatterjee, M. Dasgupta, S. Kailas, R.C. Lemmon, K. Mahata, R.G. Pillay, E.C. Pollacco, K. Ramachandran, M. Rejmund, A. Shrivastava, J.L. Sida, E. Tryggstad. Direct and compound reactions induced by unstable helium beams near the Coulomb barrier. *Phys. Rev. C* **70**, 044601 (2004).
2. A. Chatterjee, A. Navin, A. Shrivastava, S. Bhattacharyya, M. Rejmund, N. Keeley, V. Nanal, J. Nyberg, R.G. Pillay, K. Ramachandran, I. Stefan, D. Bazin, D. Beaumel, Y. Blumenfeld, G. de France, D. Gupta, M. Labiche, A. Lemasson, R. Lemmon, R. Raabe, J.A. Scarpaci, C. Simenel, C. Timis. $1n$ and $2n$ transfer with the Borromean nucleus ${}^6\text{He}$ near the Coulomb barrier. *Phys. Rev. Lett.* **101**, 032701 (2008).
3. A. Lemasson, A. Navin, N. Keeley, M. Rejmund, S. Bhattacharyya, A. Shrivastava, D. Bazin, D. Beaumel, Y. Blumenfeld, A. Chatterjee, D. Gupta, G. de France, B. Jacquot, M. Labiche, R. Lemmon, V. Nanal, J. Nyberg, R.G. Pillay, R. Raabe, K. Ramachandran, J.A. Scarpaci, C. Simenel, I. Stefan, C.N. Timis. Reactions with the double-Borromean nucleus ${}^8\text{He}$. *Phys. Rev. C* **82**, 044617 (2010).
4. F.A. Majeed, F.A. Mahdi. Quantum mechanical calculations of a fusion reaction for some selected halo systems. *Ukr. J. Phys.* **64**, 11 (2019).
5. A.A. Kulko, N.A. Demekhina, R. Kalpakchieva, N.N. Kolesnikov, V.G. Lukashik, Yu E. Penionzhkevich, D.N. Rasadov, N.K. Skobelev. Isomeric ratios for ${}^{196,198}\text{Tl}$ and ${}^{196,198}\text{Au}$ from fusion and transfer in the interaction of ${}^6\text{He}$ with ${}^{197}\text{Au}$. *J. Phys. G: Nucl. Part. Phys.* **34**, 2297 (2007).
6. R. Wolski, I. Martel, L. Standylo, L. Acosta, J.L. Agudo, C. Angulo, R. Berjillos, J.P. Bolivar, J.A. Duenas, M.S. Golovkov, T. Keutgen, M. Mazzocco, A. Padilla, A.M. Sánchez-Benítez, C. Signorini, M. Romoli, K. Rusek. Sub-barrier fusion of ${}^6\text{He}$ with ${}^{206}\text{Pb}$. *Eur. Phys. J. A* **47**, 111 (2011).
7. S.M. Lukyanov, Yu.E. Penionzhkevich, R.A. Astabatiev, N.A. Demekhina, Z. Dlouhy, M.P. Ivanov, R. Kalpakchieva, A.A. Kulko, E.R. Markarian, V.A. Maslov, R.V. Revenko, N.K. Skobelev, V.I. Smirnov, Yu.G. Sobolev, W. Trazska, S.V. Khlebniko. Study of the $2n$ -evaporation channel in the ${}^4,6\text{He} + {}^{206,208}\text{Pb}$ reactions. *Phys. Lett. B* **670**, 321 (2009).
8. A. Lemasson, A. Shrivastava, A. Navin, M. Rejmund, N. Keeley, V. Zelevinsky, S. Bhattacharyya, A. Chatterjee, G. de France, B. Jacquot, V. Nanal, R. G. Pillay, R. Raabe, C. Schmitt. Modern Rutherford experiment: Tunneling of the most neutron-rich nucleus. *Phys. Rev. Lett.* **103**, 232701 (2009).
9. V.V. Parkar, G. Marquinez, I. Martel, A.M. Sánchez-Benítez, L. Acosta, R. Berjillos, J. Duecas, J.L. Flores, J.P. Bolívar, A. Padilla, M.A.G. Alvarez, D. Beaumel, M.J.G. Borge, A. Chbihi, C. Cruz, M. Cubero, J.P. Fernández Garcia, B. Fernández Martínez, J. Gomez Camacho, N. Keeley, J.A. Labrador, M. Marquis, M. Mazzocco, A. Pakou, N. Patronis, V. Pesudo, D. Pierroutsakou, R. Raabe, K. Rusek, R. Silvestri, L. Standylo, I. Strojek, N. Soic, O. Tengblad, R. Wolski, A.H. Ziad. Fusion of ${}^8\text{He}$ with ${}^{206}\text{Pb}$ around Coulomb barrier energies. *EPJ Web of Conferences* **17**, 16009 (2011).
10. G.R. Satchler, W.G. Love. Folding model potentials from realistic interactions for heavy-ion scattering. *Phys. Rep.* **55**, 183 (1979).
11. J.W. Negele. The mean-field theory of nuclear structure and dynamics. *Rev. Mod. Phys.* **54**, 913 (1982).
12. D. Vautherin, D.M. Brink. Hartree-Fock calculations with Skyrme's interaction. I. Spherical nuclei. *Phys. Rev. C* **5**, 626 (1972).
13. K.P. Santhosh, I. Sukumaran. Alpha decay studies on Po isotopes using different versions of nuclear potentials. *Eur. Phys. J. A* **53**, 246 (2017).
14. R. Gharaei, V. Zanganeh. Temperature-dependent potential in cluster-decay process. *Nucl. Phys. A* **952**, 28 (2016).
15. K. Manimaran, M. Balasubramaniam. Deformation and orientation effects in the ternary fragmentation potential of the ${}^4\text{He}$ - and ${}^{10}\text{Be}$ -accompanied fission of the ${}^{252}\text{Cf}$ nucleus. *J. Phys. G, Nucl. Part. Phys.* **37**, 045104 (2010).
16. M Aygun. Alternative potentials analyzing the scattering cross-sections of ${}^{7,9,10,11,12,14}\text{Be}$ isotopes from a ${}^{12}\text{C}$ target: proximity potentials. *J. Korean Phys. Soc.* **73**, 1255 (2018).

17. M Aygun. A comparison of proximity potentials in the analysis of heavy-ion elastic cross-sections. *Ukr. J. Phys.* **63**, 881 (2018).
18. M Aygun. The application of some nuclear potentials for quasielastic scattering data of the $^{11}\text{Li} + ^{28}\text{Si}$ reaction and its consequences. *Turk. J. Phys.* **42**, 302 (2018).
19. M Aygun. Comparative analysis of proximity potentials to describe scattering of ^{13}C projectile off ^{12}C , ^{16}O , ^{28}Si and ^{208}Pb nuclei. *Rev. Mex. Fis. E* **64**, 149 (2018).
20. J. Błocki, J. Randrup, W.J. Świątecki, C.F. Tsang. Proximity forces. *Ann. Phys. (NY)* **105**, 427 (1977).
21. I. Dutt, R.K. Puri. Comparison of different proximity potentials for asymmetric colliding nuclei. *Phys. Rev. C* **81**, 064609 (2010).
22. W.D. Myers, W.J. Świątecki. Nuclear masses and deformations. *Nucl. Phys.* **81**, 1 (1966).
23. P. Möller, J.R. Nix. Macroscopic potential-energy surfaces for symmetric fission and heavy-ion reactions. *Nucl. Phys. A* **272**, 502 (1976).
24. H.J. Krappe, J.R. Nix, A.J. Sierk. Unified nuclear potential for heavy-ion elastic scattering, fusion, fission, and ground-state masses and deformations. *Phys. Rev. C* **20**, 992 (1979).
25. P. Möller, J.R. Nix. Nuclear mass formula with a Yukawa-plus-exponential macroscopic model and a folded-Yukawa single-particle potential. *Nucl. Phys. A* **361**, 117 (1981).
26. G. Royer, B. Remaud. On the fission barrier of heavy and superheavy nuclei. *J. Phys. G: Nucl. Part. Phys.* **10**, 1541 (1984).
27. W. Reisdorf. Heavy-ion reactions close to the Coulomb barrier. *J. Phys. G, Nucl. Part. Phys.* **20**, 1297 (1994).
28. R. Kumar. Effect of isospin on the fusion reaction cross section using various nuclear proximity potentials within the Wong model. *Phys. Rev. C* **84**, 044613 (2011).
29. P. Moller, J.R. Nix, W.D. Myers, W.J. Swiatecki. Nuclear ground-state masses and deformations. *At. Data Nucl. Data Tables* **59**, 185 (1995).
30. K. Pomorski, J. Dudek. Nuclear liquid-drop model and surface-curvature effects. *Phys. Rev. C* **67**, 044316 (2003).
31. I. Dutt, R.K. Puri. Role of surface energy coefficients and nuclear surface diffuseness in the fusion of heavy-ions. *Phys. Rev. C* **81**, 047601 (2010).
32. R. Gharaei, V.Zanganeh, N. Wang. Systematic study of proximity potentials for heavy-ion fusion cross sections. *Nucl. Phys. A* **979**, 237 (2018).
33. G.L. Zhang, Y.J. Yao, M.F. Guo, M. Pan, G.X. Zhang, X.X. Liu. Comparative studies for different proximity potentials applied to large cluster radioactivity of nuclei. *Nucl. Phys. A* **951**, 86 (2016).
34. A. Winther. Dissipation, polarization and fluctuation in grazing heavy-ion collisions and the boundary to the chaotic regime. *Nucl. Phys. A* **594**, 203 (1995).
35. R. Bass. Threshold and angular momentum limit in the complete fusion of heavy ions. *Phys. Lett. B* **47**, 139 (1973).
36. R. Bass. Fusion of heavy nuclei in a classical model. *Nucl. Phys. A* **231**, 45 (1974).
37. R. Bass. Nucleus-nucleus potential deduced from experimental fusion cross sections. *Phys. Rev. Lett.* **39**, 265 (1977).
38. P.R. Christensen, A. Winther. The evidence of the ion-ion potentials from heavy ion elastic scattering. *Phys. Lett. B* **65**, 19 (1976).
39. H. Ngô, Ch. Ngô. Calculation of the real part of the interaction potential between two heavy ions in the sudden approximation. *Nucl. Phys. A* **348**, 140 (1980).
40. V.Yu. Denisov. Interaction potential between heavy ions. *Phys. Lett. B* **526**, 315 (2002).
41. G.R. Satchler. *Direct Nuclear Reactions* (Oxford Univ. Press, 1983).
42. I.J. Thompson. Coupled reaction channels calculations in nuclear physics. *Computer Phys. Rep.* **7**, 167 (1988).

Received 09.02.19

M. Айгун

ВПЛИВ ПОТЕНЦІАЛІВ БЛИЗЬКОСТІ НА ПЕРЕРІЗ РЕАКЦІЙ СИНТЕЗУ $^{6,8}\text{He} + ^{65}\text{Cu}$ З ГАЛІО ЯДРАМИ

Резюме

Проведено повне теоретичне дослідження потенціалів близькості для найкращого опису реакцій синтезу $^{6,8}\text{He} + ^{65}\text{Cu}$. Використано такі різні потенціали: Prox 66, Prox 76, Prox 77, Prox 79, Prox 81-I, Prox 81-II, Prox 81-III, Prox 84, Prox 88, Mod-Prox-88, Prox 95, Prox 2003-I, Prox 2003-II, Prox 2003-III, Prox 2010, BW 91, AW 95, Bass 73, Bass 77, Bass 80, CW 76, Ngo 80 і D. Найкращі потенціали визначені на підставі порівняння теоретичних і експериментальних даних по реакціях $^{6,8}\text{He} + ^{65}\text{Cu}$.